

Design and Development of Biomimetic Nanovesicles Using a Microfluidic Approach


Roberto Molinaro,* Michael Evangelopoulos, Jessica R. Hoffman, Claudia Corbo, Francesca Taraballi, Jonathan O. Martinez, Kelly A. Hartman, Donato Cosco, Giosue' Costa, Isabella Romeo, Michael Sherman, Donatella Paolino, Stefano Alcaro, and Ennio Tasciotti*

The advancement of nanotechnology toward more sophisticated bioinspired approaches has highlighted the gap between the advantages of biomimetic and biohybrid platforms and the availability of manufacturing processes to scale up their production. Though the advantages of transferring biological features from cells to synthetic nanoparticles for drug delivery purposes have recently been reported, a standardizable, batch-to-batch consistent, scalable, and high-throughput assembly method is required to further develop these platforms. Microfluidics has offered a robust tool for the controlled synthesis of nanoparticles in a versatile and reproducible approach. In this study, the incorporation of membrane proteins within the bilayer of biomimetic nanovesicles (leukosomes) using a microfluidic-based platform is demonstrated. The physical, pharmaceutical, and biological properties of microfluidic-formulated leukosomes (called NA-Leuko) are characterized. NA-Leuko show extended shelf life and retention of the biological functions of donor cells (i.e., macrophage avoidance and targeting of inflamed vasculature). The NA approach represents a universal, versatile, robust, and scalable tool, which is extensively used for the assembly of lipid nanoparticles and adapted here for the manufacturing of biomimetic nanovesicles.

Recently, advances in biomimicry, i.e., the biologically inspired design of materials,^[1] has spurred the development of novel strategies to bestow nano- and microparticles with multiple functionalities necessary to negotiate biological barriers.^[2] Current approaches for drug delivery carriers include mimicking of leukocytes,^[3] red blood cells (RBCs),^[4] platelets,^[5] and cancer cells^[6] to achieve superior delivery of therapeutics compared to conventional nanoparticles. These hybrid biomimetic carriers showed advantageous pharmaceutical properties (i.e., defined size and shape, physical stability, ability to load and release chemically different therapeutics) resulting from the synthetic backbone materials (nanoporous silicon,^[3a] phospholipids,^[3b] and poly(lactic-co-glycolic) acid^[7]) they were derived from. Furthermore, these biomimetic strategies demonstrated innate biological features and intrinsic functionalities (long circulation, selective targeting toward

Dr. R. Molinaro,^[†] M. Evangelopoulos, J. R. Hoffman, Dr. C. Corbo, Dr. F. Taraballi, Dr. J. O. Martinez, K. A. Hartman, Dr. E. Tasciotti,^[††]
Center of Biomimetic Medicine
Houston Methodist Research Institute
6670 Bertner Avenue, Houston, TX 77030, USA
E-mail: rmolinaro@bwh.harvard.edu;
etasciotti@houstonmethodist.org

Dr. R. Molinaro
Nanoinspired Biomedicine Lab
Fondazione Istituto di Ricerca
Pediatria Città della Speranza
35127 Padua, Italy

 The ORCID identification number(s) for the author(s) of this article can be found under <https://doi.org/10.1002/adma.201702749>.

^[†]Present address: Department of Cardiovascular Medicine, Harvard Medical School, Brigham and Women's Hospital, 77 Avenue Louis Pasteur, Boston, MA 02115, USA

^[††]Present address: Department of Orthopedics and Sports Medicine, Houston Methodist Hospital, 6565 Fannin Street, Houston, TX 77030, USA

Dr. D. Cosco, Dr. G. Costa, I. Romeo, Dr. S. Alcaro
Department of Health Sciences
University "Magna Græcia" of Catanzaro
Campus Universitario "S. Venuta,"
Viale S. Venuta, Germaneto, I-88100 Catanzaro, Italy

Dr. M. Sherman
Department of Biochemistry and Molecular Biology
Sealy Center for Structural Biology and Molecular Biophysics
University of Texas Medical Branch
Galveston, TX 77555, USA

Dr. D. Paolino
Department of Experimental and Clinical Medicine
University "Magna Græcia" of Catanzaro
Campus Universitario "S. Venuta,"
Viale S. Venuta, Germaneto, I-88100 Catanzaro, Italy

Dr. E. Tasciotti
Houston Methodist Orthopedic and Sports Medicine
Houston Methodist Hospital
6565 Fannin Street, Houston, TX 77030, USA

DOI: 10.1002/adma.201702749

specific biological compartments) typical of the donor cell source.^[8] When investigating the events occurring at the nano–bio interface, e.g., the protein corona formation,^[9] a distinctive interaction of these biomimetic carriers with blood components compared to their non-biomimetic counterpart can be observed.^[10] Using this approach, leukocyte-like nanovesicles showed prolonged circulation and preferential targeting of inflamed vasculature,^[3b] while platelet-like nanoparticles displayed platelet-mimicking properties such as adhesion to damaged vasculature and binding to platelet-adhering pathogens.^[5] However, the new biological functionalities transferred to these hybrid nanomaterials increased their degree of complexity from a regulatory standpoint. Nanomaterials for biomedical applications must account for or develop methods to ensure that final products are standardized, batch-to-batch consistent, scalable, good manufacturing practice (GMP)-compliant, and amendable to high-throughput assembly methods. As a matter of fact, the difficulty of producing nanoparticles in a standardized and reproducible way in sufficient quantities has hindered their successful translation to clinical applications. However, despite current protocols addressing several hurdles, such as (i) retention of biological complexity of cellular membrane on carrier surface, (ii) control of physicochemical properties over the final formulation, (iii) customizability, and (iv) stability, a major challenge remains in the development of adequate protocols for scaling up the manufacturing of nanoparticles.^[11]

In response to this need, microfluidics—the science of manipulating fluids at the micrometer or smaller scale in a controlled fashion^[12]—emerged as a promising technique allowing for the controlled synthesis of nanoparticles providing a versatile method to accelerate their transition to the clinic.^[11] From a technical standpoint, the concept behind microfluidics is that a change in solvent polarity can drive the self-assembly of lipids or other amphiphilic molecules.^[13] By controlling the flow rate ratio (FRR) between the aqueous and organic phases, the total flow rate (TFR) of the two streams, and the temperature, it is possible to tune the final size and distribution of resulting nanoparticles^[11,14] as well as their drug loading capacity and batch-to-batch reproducibility.^[13,15] Recently, a microfluidic-based platform, called NanoAssemblr (NA) (Figure 1a), has been developed for the manufacture of nanoparticles in a controlled, tunable, low-cost, and scalable fashion.^[16] The mixing process in the microfluidic mixing chamber of the NA is achieved through the combination of a Y-shaped inlet channel and the inclusion of microstructures, so-called herringbone mixers.^[17] The herringbone micromixer induces chaotic advection, which allows for the stretching and folding of fluid streams over the channels' cross-sectional area. This, together with the herringbone structures of the channel floor, increases mass transfer under laminar flow conditions.^[18] The repeated folding of two miscible fluids under laminar flow allows for extremely fast mixing (millisecond mixing) of the two fluids under mild conditions (low shear, low heat, and low pressure) and prevents the occurrence of uncontrolled solvent gradients. The adjustment of mixing ratio, flow rate, and lipid composition allowed for the fine-tuning of physical features of lipid nanoparticles for the delivery of adjuvants and siRNA.^[19]

Herein, we show, for the first time, a continuous-based process to incorporate membrane proteins derived from leukocytes within the lipid bilayer of liposome-like nanovesicles (i.e., leukosomes) using NA technology. This study represents a

proof-of-principle investigation of the versatile, reproducible, robust and high-throughput manufacture of biomimetic nanovesicles using a microfluidic-based synthetic protocol. NA-formulated leukosomes (NA-Leuko) have been fully characterized for their physical and pharmaceutical properties. In addition, the successful transfer of biological features to NA-Leuko has been validated using both *in vitro* and *in vivo* models.^[3b]

The first step in optimizing NA-Leuko assembly consisted of tailoring mixing protocols to generate stable nanovesicles suitable for additional membrane protein incorporation in terms of average diameter, size homogeneity, and zeta potential. By tuning FRR (1:1, 2:1, and 3:1 aqueous-to-organic phase), TFR (1, 3, 6, 9, and 12 mL min⁻¹), and operating temperature (room temperature versus 45 °C, data not shown), we identified that 2:1 FRR, 1 mL min⁻¹ TFR, and 45 °C gave the best conditions for membrane protein incorporation. Liposomes produced with these settings showed a mean diameter of 118 nm, a polydispersity index (PDI) of 0.13, and surface charge of -12 mV (Figure 1). The incorporation of membrane proteins at increasing protein-to-lipid ratios (from 1:300, 1:100, to 1:50) induced a slight reduction of the mean diameter of the resulting proteolipid vesicles, i.e., from 118 nm (control liposomes) to 103, 104, and 94 nm, respectively (Figure 1b), while significantly affecting their surface charge (Figure 1c). Contrarily to observations using the thin layer evaporation (TLE) method,^[3b] protein integration into the lipid bilayer produced a relative decrease of surface charge (e.g., -9, -21, and -27 mV, respectively) that, in the case of NA-Leuko, was proportional to the increase in the protein-to-lipid concentration (Figure 1c). A minor increase in PDI (<0.2 for all protein-to-lipid ratios) following protein incorporation, instead, was observed (Figure 1b), revealing a high size homogeneity for these formulations. Size homogeneity was also confirmed by low-magnification cryoEM analysis (see Figure S1 in the Supporting Information). It is worth noting that the above-mentioned values result from the average of at least three different batches of independently synthesized particles, which reveal the high reproducibility of this method, as previously reported by others.^[20] To further confirm the small batch-to-batch variations, we evaluated the reproducibility of NA-Leuko assembled (i.e., size distribution) by three different operators. As reported in Figure S2 (Supporting Information), the maximum variability observed among three individual operators was 2.5%, indicating consistent reproducibility of NA-Leuko.

Next, we performed the extrusion assay to determine the successful incorporation of membrane proteins within the lipid bilayer. As previously described by our group,^[3b] we observed a direct correlation between the bilayer transition temperature (T_m) and its physical deformability, following protein integration within a lipid bilayer. We found that the increase of T_m , which is directly related to the increase of membrane protein incorporation, corresponded to a reduction of bilayer deformability. In other words, the higher the protein incorporation, the more rigid the lipid bilayer, and the less deformable the vesicles. As shown in Figure 1d, we observed a reduction of vesicle deformability, expressed as the deformability index (DI), proportional to the increase of protein concentration in the following order: 1:50 < 1:100 < 1:300. While statistical significance was calculated upon increasing protein-to-lipid ratio from 1:300 to 1:50, we found the most optimal ratio to be 1:50, as a plateau was eventually reached at higher concentrations, indicating minimal

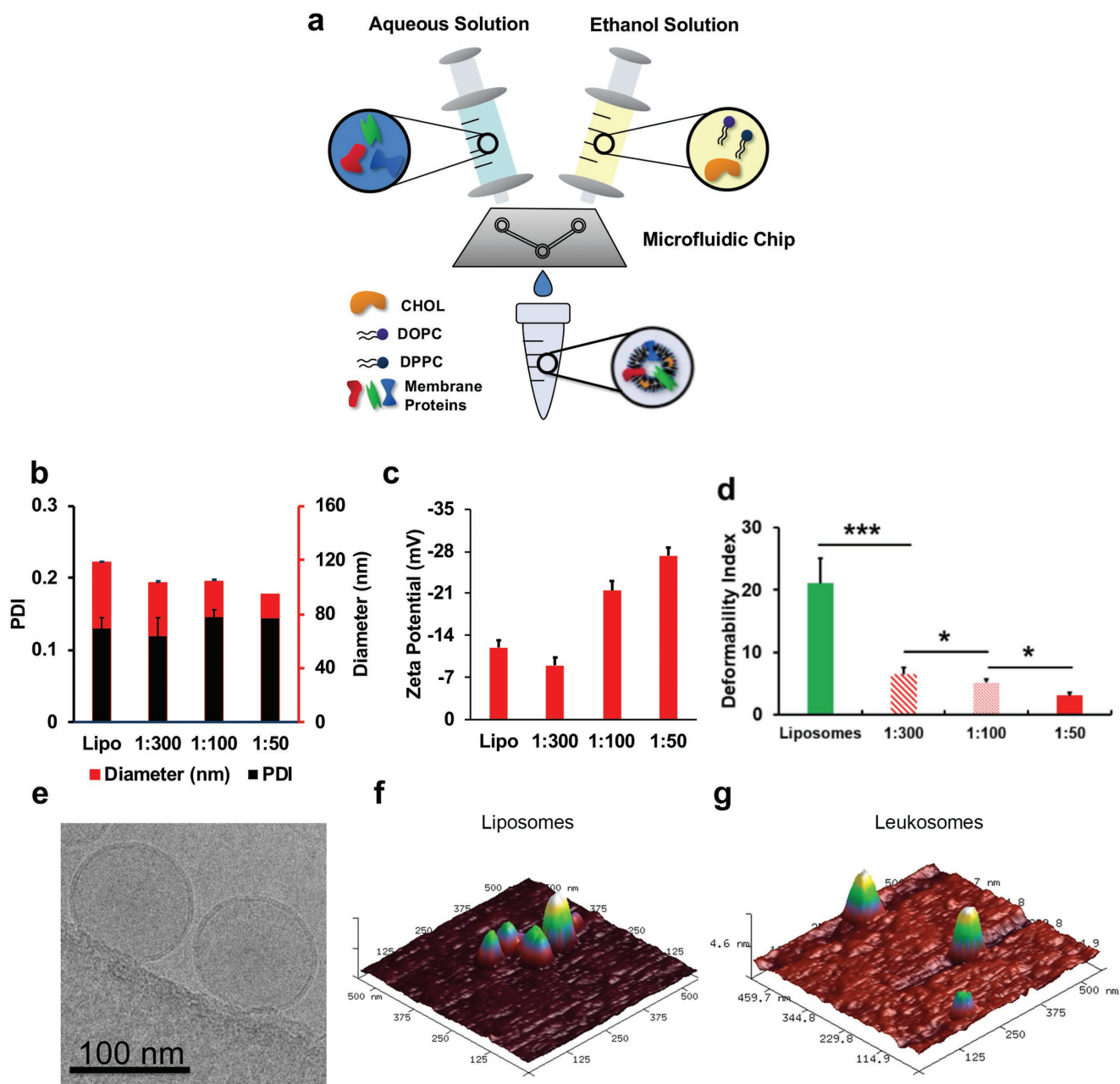


Figure 1. Continuous-based process for the assembly of biomimetic nanovesicles using NanoAssemblr platform. a) Schematic representation of leukosomes microfluidic synthesis (not to scale). b) Dynamic light scattering (DLS) analysis shows average diameter, polydispersity index (PDI), and c) zeta potential of liposomes (Lipo) and NA-Leuko after membrane protein incorporation at 1:300, 1:100, and 1:50 protein-to-lipid ratios. d) Deformability index shows vesicles' flexibility following to membrane proteins incorporation at 1:300, 1:100, and 1:50 protein-to-lipid ratios, and identifies the 1:50 ratio as the highest level of protein incorporation. Results represent the average of at least three different batches of particles \pm standard deviation. e) High-magnification cryoEM analysis of 1:50 NA-Leuko reveals spherical shape, unilamellar vesicles, and validates DLS analysis. f) Liposome and g) NA-Leuko surface profile using atomic force microscopy (AFM) analysis. $**p < 0.1$; $***p < 0.01$; $****p < 0.001$.

gain from the increased protein composition. Taken together, these findings reveal that 1:50 protein-to-lipid ratio represents the highest level of protein incorporation and, as per these results, 1:50 protein-to-lipid ratio was selected as the best ratio for further studies. The evaluation of the percentage of protein incorporation into the bilayer of three independently assembled NA-Leuko revealed that, compared to the TLE method^[3b]

(protein incorporation efficiency of 63%), around 90% of the membrane proteins initially added to the aqueous stream are associated with the final formulation (see Figure S3 in the Supporting Information). In addition, theoretical calculations based on established criteria performed on NA-Leuko versus TLE-Leuko (see the Supporting Information) showed (i) a 2.18-fold increase of the total number of nanovesicles per gram of lipid;

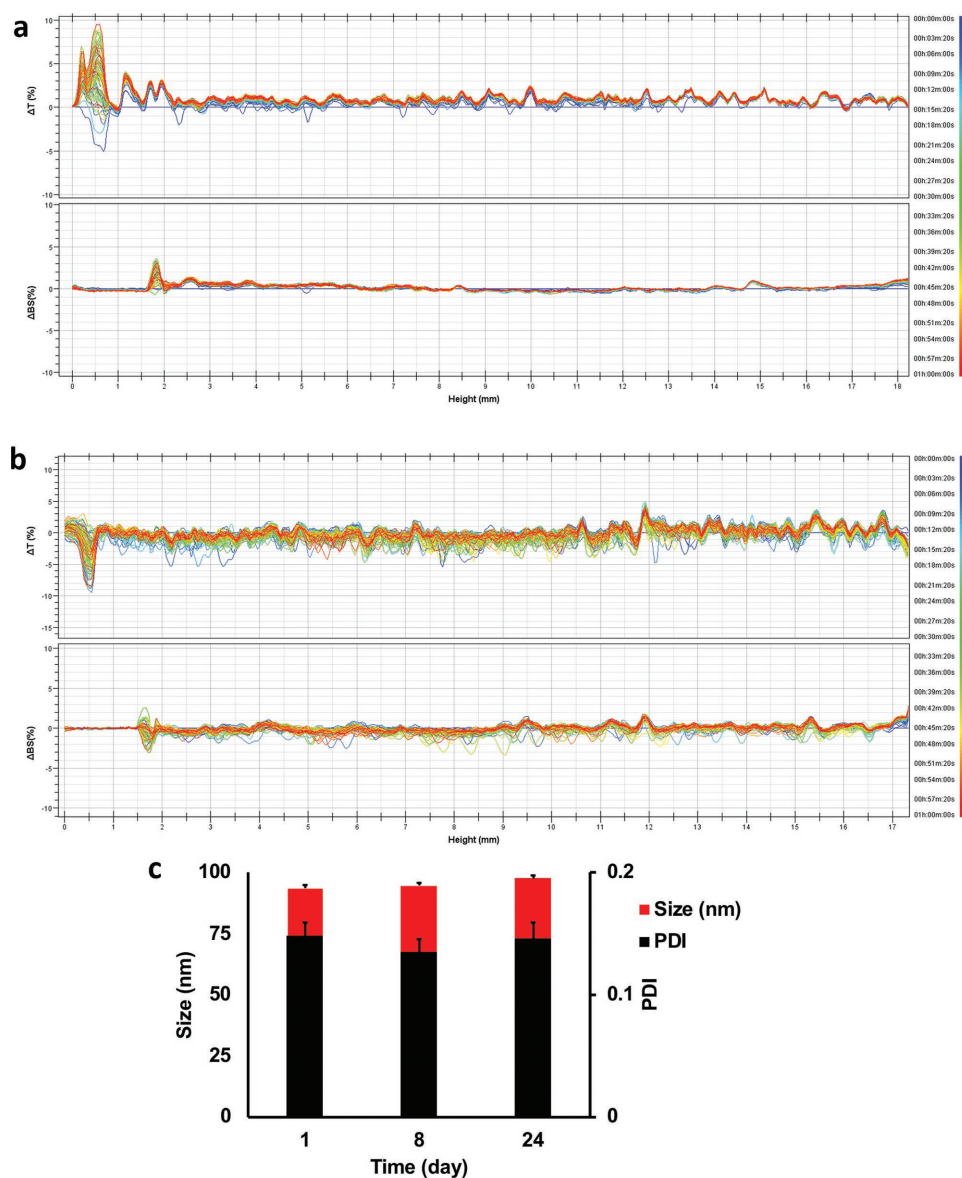


Figure 2. Physical stability of biomimetic NA-Leuko. Transmission (ΔT %) and backscattering (ΔBS %) profiles of a) liposomes and b) NA-Leuko using Turbiscan Lab. The analysis was performed at 20 °C. Data are reported as a function of time (0–1 h) and sample height (from 2 to 15 mm). c) DLS analysis of NA-Leuko stored in solution at 4 °C up to 24 d reveals no significant change in size and homogeneity.

(ii) a 14-fold increase of membrane proteins into the NA-Leuko bilayer with respect to TLE-Leuko; and (iii) a 22.7-fold increase of membrane proteins per μm^2 of surface area for NA-Leuko compared to TLE-Leuko (see Figure S4 in the Supporting Information). Inspection of cryoEM images of NA-Leuko at this ratio revealed spherical shape and unilamellarity (Figure 1e). Atomic force microscopy (AFM) analysis validated the size of the particles as measured with dynamic light scattering (DLS) and cryoEM (Figure 1f,g). Additional AFM analysis showed increased roughness and elasticity for NA-Leuko compared to control liposomes (see Figure S5 in the Supporting Information), but similar to TLE leukosomes (TLE-Leuko).^[3b]

The physical stability of NA-Leuko was evaluated for pharmaceutical purposes through Turbiscan Lab.^[21] Widely used in the pharmaceutical field, this method uses the multiple

light scattering principle to detect any instability phenomena of colloidal systems (e.g., flocculation, sedimentation, and coagulation) through the analysis of photons scattered (delta backscattering, ΔBS) or transmitted (delta transmittance, ΔT) from the sample over time.^[21,22] We observed that ΔBS and ΔT profiles are lower than $\pm 5\%$ for both control liposomes and NA-Leuko at 20 °C, thus indicating long-term shelf life^[23] (Figure 2a,b). To support this finding, NA-Leuko were stored in solution at 4 °C up to 24 d and their size was measured over time. DLS analysis revealed minimal changes in diameter and size homogeneity (Figure 2c). In addition, the evaluation of the turbiscan stability index revealed similar profiles between the two formulations at both 20 and 37 °C, thus confirming that proteins incorporation had no unfavorable effect on the stability of NA-Leuko (see Figure S6 in the Supporting Information).

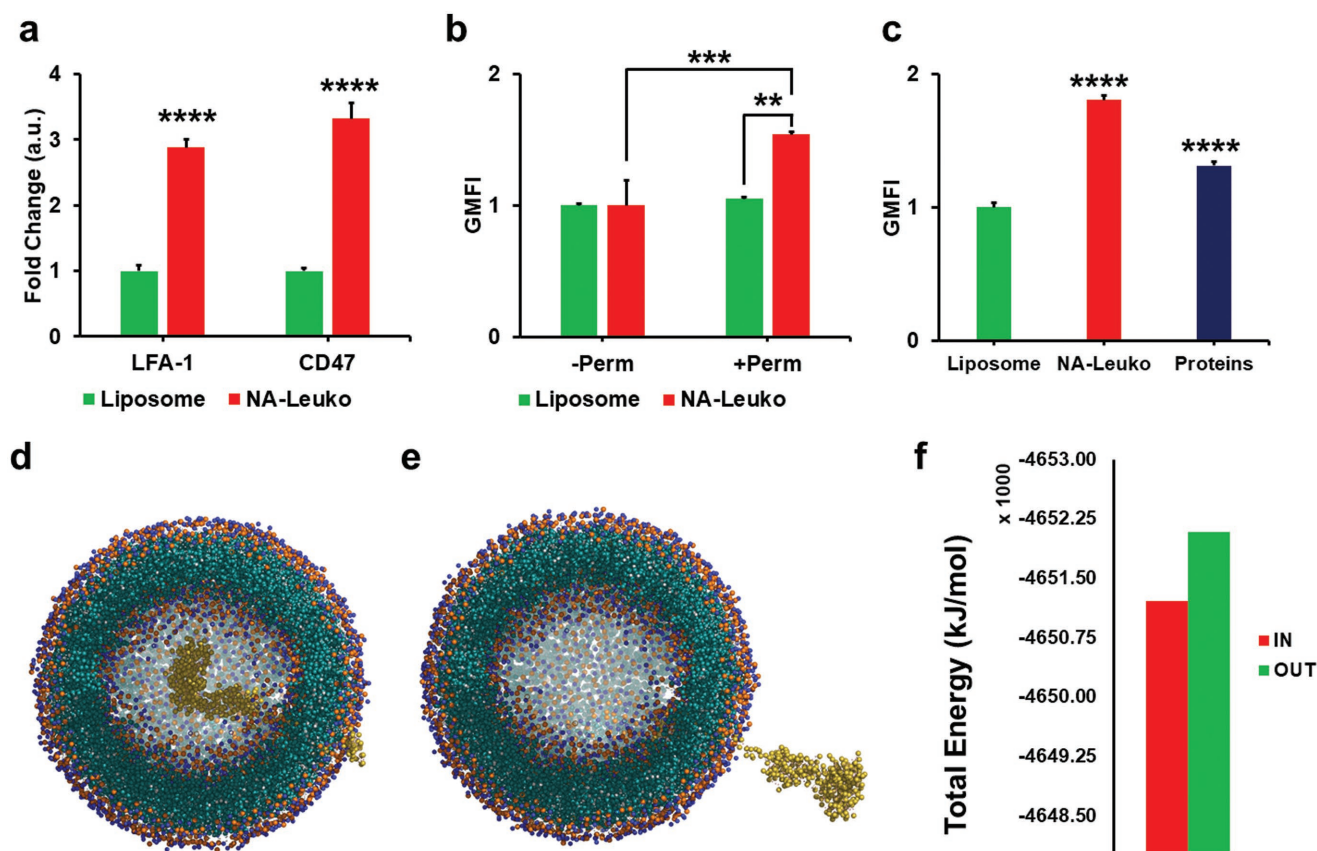


Figure 3. Orientation of membrane proteins within the bilayer of NanoAssemblr-derived leukosomes (NA-Leuko). Flow cytometry analysis performed on liposomes and NA-Leuko revealed a) the presence and correct orientation of LFA-1 and CD47 on NA-Leuko surface, b) the absence of signal from intracellular domains CD3z of membrane proteins, and c) the presence of glycosylated domains on NA-Leuko surface and self-assembled membrane proteins (positive control). d) The coarse-grained model represents 3D structure of the integral protein MHC I in the orientation OUT, i.e., glycosylated domain oriented outside NA-Leuko bilayer, and e) IN, glycosylated domain oriented inside NA-Leuko bilayer, respectively. f) Total energy calculated as difference between the energies relative to the outside and inside orientations, identified as OUT and IN, respectively, of the glycosylated domain of the integral protein MHC I. The energy values are reported in kJ mol^{-1} , indicated in a range between -4649 and $-4653 \times 10^3 \text{ kJ mol}^{-1}$. $**p < 0.1$; $***p < 0.01$; and $****p < 0.001$.

To evaluate the impact of microfluidic manipulation on the orientation of proteins within NA-Leuko bilayer, we confirmed the exposure of the extracellular domains of LFA-1 and CD47 on the surface of NA-Leuko (Figure 3a). In addition, analysis of CD3z^[3a] revealed the absence of intracellular domains of membrane proteins exposed on the outer leaflet of NA-Leuko bilayer (Figure 3b). As for control liposomes, no significant difference was observed in CD3z signal, while after bilayer permeabilization using 0.01% Tween 80, we observed an increase in CD3z signal only for NA-Leuko (Figure 3b). Further assays were carried out to detect the presence of any contaminants in NA-Leuko formulation. Flow cytometry analysis did not detect p62 and COX IV markers, representative of nuclear and mitochondrial contaminants, respectively (see Figure S7a in the Supporting Information). In addition, no statistically significant difference between liposomes and NA-Leuko was observed after 4',6-diamidino-2-phenylindole (DAPI) incubation, confirming the absence of contamination from nucleic acids (see Figure S7b in the Supporting Information). Wheat germ agglutinin assay revealed the presence of glycosylated domains of membrane proteins (Figure 3c), suggesting both the retention of post-translational modifications as well as the correct

orientation of the surface proteins. While proteins incorporation within a lipid bilayer may at first appear random, we proposed that various factors, like glycosylation,^[3b,24] the steric hindrance of the protein extracellular domain versus the intracellular domain, and relative to vesicle curvature, are critical factors that drive their correct orientation. We tested our hypothesis performing in silico analysis using a simplified system that simulates the thermodynamic profile of an integral protein within the lipid bilayer of a leukosome. The computational analysis does not directly demonstrate the dynamics beyond the orientation of the membrane proteins into the NA-Leuko bilayer, but supports theoretically the experimental findings obtained through physical characterization and flow cytometry analysis. In this scenario, the use of coarse-grained (CG) models has proven to be a valuable tool to probe the time and length scales of systems beyond what is feasible with the traditional computational models (e.g., all atomistic models).^[25] CG simulations allowed for calculating free energy barriers with similar accuracy as those from the full atomistic ones, while accelerating 500-fold the simulation, and preserving the biological relevance of the interactions.^[25] In order to discriminate the energetic component that most likely stabilized the system in one of the two

orientations, we simulated the potential scenario having the glycosylated domain exposed outside the bilayer (orientation “OUT,” see Video SV1 in the Supporting Information) or inside, toward the vesicle core (orientation “IN,” see Video SV2 in the Supporting Information). The CG model (Figure 3d,e) was very useful to evaluate the generated system not only for the low number of particles, but also for the low potential energy background, which allowed us to explore longer time lapses. The system showed the most advantageous energy profile (variation of Total Energy_{OUT/IN} of $-868.5 \text{ kJ mol}^{-1}$) when the glycosylated extracellular domain was directed outside the vesicle (orientation OUT) compared to its IN orientation (Figure 3f; Figure S8, Supporting Information). In addition, we calculated the Lennard–Jones (LJ) and Coulomb potentials (see Figures S9 and S10 in the Supporting Information) to determine the most favorable orientation. We discovered a variation of LJ_{OUT/IN} and Coulomb_{OUT/IN} potentials of $-1,041.1$ and $-36.8 \text{ kJ mol}^{-1}$, respectively, for the glycosylation domain oriented outside the vesicle (OUT) with respect to the inside (IN) orientation (see Figures S9 and S10 in the Supporting Information). From an energetic standpoint, these findings support the correct orientation of membrane proteins within NA-Leuko bilayer, and suggested that the driving forces of the process were the steric hindrance of the glycosylated domain and the significant reduction of the energetic profile when the glucidic moiety was oriented outside the vesicle.

We and others^[3b,7] have previously showed that the physical transfer of membrane proteins to synthetic carriers results in the acquisition of novel biological functions.^[8d,10] Here, we evaluated whether our microfluidic-driven synthesis preserved the biological functions of transferred membrane proteins both in vitro and in vivo. We tested in vitro the ability of NA-Leuko incorporating macrophage-derived membrane proteins to delay phagocytosis when incubated with syngeneic macrophages. Compared to control liposomes, we observed a significantly reduced uptake for NA-Leuko at 6 and 24 h using both confocal microscopy and flow cytometry (Figure 4a,b). Next, we explored if the microfluidic approach had an effect on the adhesion of human leukocyte membrane proteins toward human umbilical vein endothelial cells (HUVECs), a biological function that was conserved for TLE-Leuko.^[3b] Proteomic analysis on human NA-Leuko revealed the presence of adhesion markers responsible for NA-Leuko targeting of inflamed endothelium and identified the leukocyte trans-endothelial migration as the best represented pathway (see Figure S11 in the Supporting Information). When incubated in flow conditions with a reconstructed monolayer of tumor necrosis factor α (TNF α)-activated HUVECs, NA-Leuko showed a threefold increased adhesion compared to control liposomes (Figure 4b). No statistically significant difference in the adhesion between control liposomes and NA-Leuko groups was observed on resting (i.e., not inflamed) HUVECs (Figure 4c), thus highlighting the selectivity of NA-Leuko targeting. To evaluate if this selective inflamed targeting was conserved during systemic administration in mice, and to have a direct comparison with the biological activity of TLE-Leuko, we created a localized inflammation model by subcutaneously injecting lipopolysaccharide (LPS) into the right ear of Balb/c mice, and used the contralateral ear as an internal control permitting inspection of the selective binding of NA-Leuko to inflamed vasculature. While control liposomes did not exhibit any preferential targeting toward inflammation with no difference in

accumulation observed between the inflamed and control ears,^[3b] NA-Leuko preferentially targeted the inflamed ear at both 1 and 24 h demonstrating an increase from 8- to 13-fold in accumulation compared to non-inflamed ears, respectively (Figure 4d). In addition, targeting properties of NA-Leuko were retained over time and could translate to similar drug delivery features as TLE-Leuko. Taken together, these findings reveal the crucial contribution of membrane proteins to the biological properties of these biomimetic nanovesicles in terms of both delay of macrophage uptake and targeting of inflamed endothelium.

Biomimetic nanoparticles represent promising new generation of drug delivery systems.^[26] In this scenario, assembly methods shifted from the manipulation of the whole cell membrane,^[5] to its fragmentation in patches^[3a] or single membrane proteins,^[3b] up to the formulation of hybrid particles by combining cell membranes from two different cells.^[27] However, despite several attempts to establish an assembly method capable of formulating clinical-grade nanoparticles, the scale-up manufacturing process still represents a major challenge for their clinical translation.^[28] The approach we report herein meets this increasing interest in the field and provides a promising tool for overcoming those limitations. Microfluidic platforms offer a high-throughput, low-cost, and scalable tool for the design and production of nanoparticles in a reproducible and standardizable fashion.^[14] For the first time, we have successfully adapted the microfluidic-based NanoAssemblr platform for the reproducible, robust, and versatile synthesis of biomimetic nanoparticles. The use of this platform includes several advantages such as: (i) accessibility and ease of use, (ii) extensive validation with respect to batch-to-batch reproducibility, (iii) automation, which allows for an easy transfer of synthetic protocol, and (iv) scalability which allows the manufacturing of nanoparticles under current GMP conditions. The resulting formulation revealed suitable pharmaceutical features, i.e., high size homogeneity, unilamellarity, as well as physical stability both at shelf-life and body temperature conditions. Membrane proteins derived from leukocytes were successfully incorporated in their correct orientation and glycosylated, post-translational status. In silico conformational analysis supported our hypothesis that glycosylation sites are responsible for the correct protein orientation within the lipid bilayer of nanovesicles. In addition, in vitro and in vivo biological analyses revealed how NA manufacturing protocols did not affect the function of the key membrane proteins, permitting the avoidance of macrophage uptake and promoting the adhesion to inflamed endothelium. In particular, compared to the previous TLE method,^[3b] the NA procedure allowed for 14-fold increase of protein concentration on the surface of leukosomes, enabling a 1.6-fold increase in vivo accumulation of NA-Leuko at the site of inflammation. Taken together, these findings support the use of this system for the scalability of biomimetic nanovesicles, thus reducing manufacturing-related costs while increasing yield and consistency.

Experimental Section

Materials: The NanoAssemblr platform (Precision NanoSystems, Inc., Vancouver, Canada) was used for incorporating leukocyte membrane proteins in lipid nanovesicles (Figure 1a). The lipids used in this study, 1,2-dipalmitoyl-*sn*-glycero-3-phosphocholine (DPPC), 1,2-dioleoyl-*sn*-glycero-3-phosphocholine (DOPC), and cholesterol, were purchased

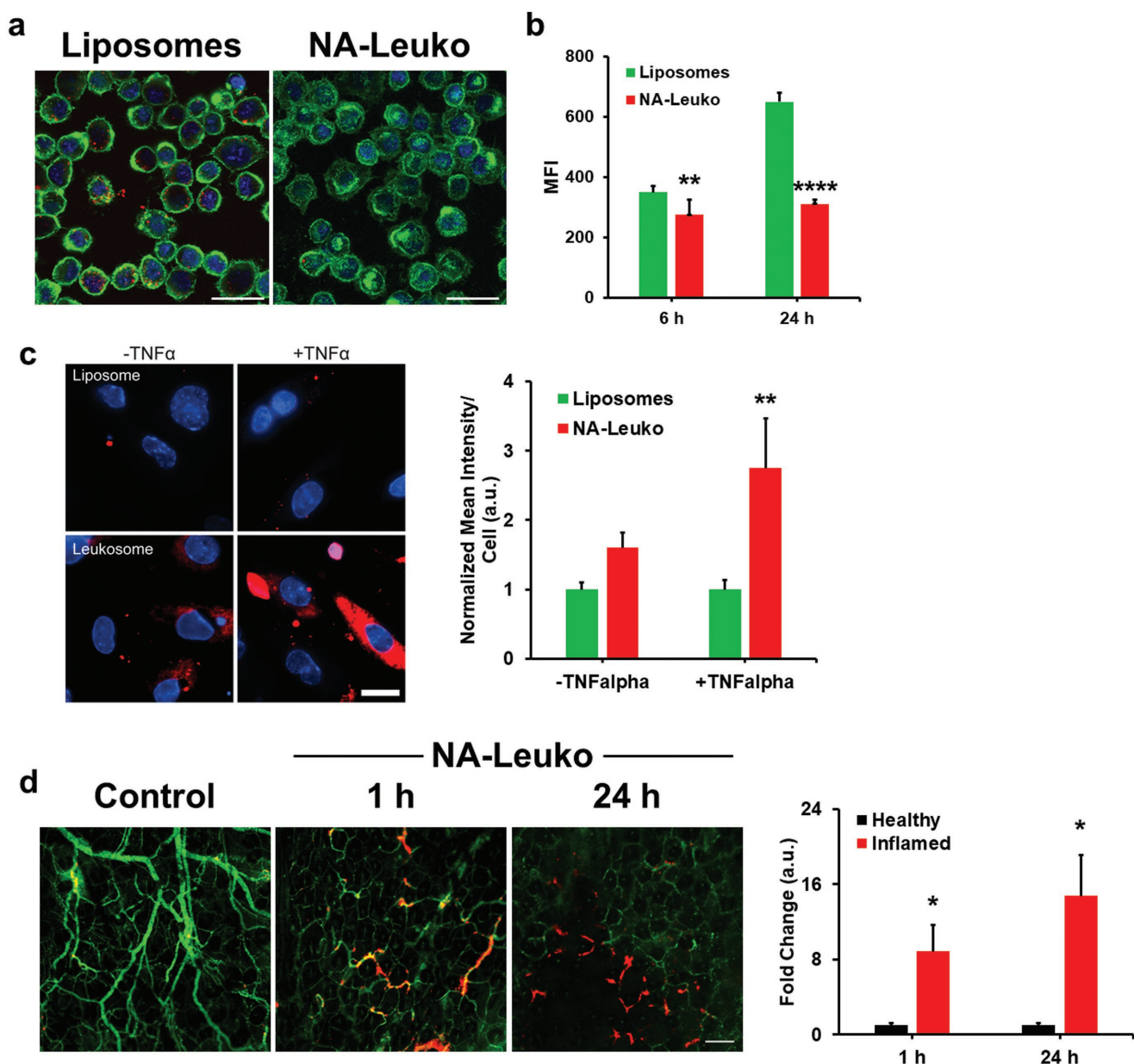


Figure 4. In vitro and in vivo biological properties of NA-Leuko. In vitro uptake studies of control liposomes and murine NA-Leuko following incubation with J774 macrophages using a) confocal microscopy (24 h incubation) and b) flow cytometry (6 and 24 h incubation). Both the techniques showed reduced phagocytosis for the biomimetic nanovesicles. Scale bar is 25 μm . Green: cell membranes stained with FITC-labeled wheat germ agglutinin; Blue: nuclei stained with DAPI; Red: particles labeled with rhodamine. c) Dynamic flow chamber experiments study the adhesion of control liposomes and NA-Leuko toward human umbilical vein endothelial cells (HUVECs). d) In vivo inflammatory targeting of NA-Leuko in a localized (i.e., ear) inflammation model ($n = 8\text{--}12$ images from three mice, graphs represent the means \pm s.e.m.). Representative IVM images show preferential accumulation of NA-Leuko in inflamed ears at 1 and 24 h with minimal accumulation observed in healthy ears. Vessels are shown in green and NA-Leuko in red; scale bar is 200 μm . Quantification revealed an 8- and 13-fold increased accumulation of NA-Leuko into the inflamed ear compared to healthy ears at both 1 and 24 h after injection, respectively. * $p < 0.05$; ** $p < 0.01$; and **** $p < 0.0001$.

from Avanti Polar Lipids, Inc., (Alabaster, AL, USA) (purity > 99%). HPLC-grade solvents were purchased from Fisher Scientific (Leicestershire, UK). Antibodies for flow cytometry (FITC-labeled anti-LFA-1, PerCP-labeled anti-CD45, COX IV, p62, and WGA) were obtained from BD Biosciences. CD3z antibody was purchased from Santa Cruz.

Membrane Protein Extraction and Incorporation within Lipid Bilayers Using Microfluidic Mixer: Biological studies aimed to prove that NA-Leuko biological properties were performed in syngeneic conditions. Leukocytes

from human blood and immortalized J774 murine macrophages^[3b] were used to assemble human and murine nanovesicles (NA-Leuko) for studies involving either human (in vitro) or murine (in vitro and in vivo) settings, respectively. While murine membrane proteins were obtained from the immortalized J774 macrophage cell line as previously shown,^[3] human membrane proteins were extracted from whole blood leukocytes, isolated following RBC lysis and centrifugation as reported from other investigators.^[29]

Phosphocholine-based phospholipids (DPPC and DOPC) and cholesterol (4:3:3 molar ratio) were dissolved in ethanol at a final lipid concentration of 9×10^{-3} M and loaded in the organic phase inlet (Figure 1, ethanol solution syringe). Membrane proteins, instead, were resuspended in aqueous buffer at 1:50, 1:100, or 1:300 protein-to-lipid concentrations and loaded in the second inlet (Figure 1, aqueous solution syringe). Before to proceed to membrane proteins incorporation, aqueous buffer and the ethanol solution of lipids were mixed at different flow rates (TFR) and flow ratios (FRR) between the two inlet streams to identify the conditions leading to the most consistent formulations in terms of size, size homogeneity, stability, and protein incorporation. Once prepared, formulations were purified from ethanol content by either dialysis or ultracentrifugation methods. Control liposomes were assembled with the NanoAssemblr Benchtop platform using the following settings: 2:1 FRR, 1 mL min⁻¹ TFR, and 45 °C; see the Supporting Information for physical characterization of NA-Leuko and computational model analysis. Experiments were performed on at least three different batches of independently synthesized particles.

In Vitro Adhesion of Human NA-Leuko to a Reconstructed Endothelium in Flow Condition: Adhesion experiments using HUVECs were carried out using human NA-Leuko.

Rhodamine-labeled NA-Leuko and liposomes, resuspended in EBM-2 media, were then infused into the slides containing HUVECs using a Harvard Apparatus PHD 2000 Infusion syringe pump at a speed of 100 μ L min⁻¹ for 30 min. After infusion, cells were washed in PBS then fixed for 10 min using 4% paraformaldehyde at room temperature. The nuclei were stained for 1 min with a PBS solution containing DAPI and washed to remove any free DAPI. Cells were imaged using an inverted Nikon Eclipse Ti fluorescence microscope equipped with a Hamamatsu ORCA-Flash 2.8 digital camera.

In Vivo Inflamed Endothelium Targeting of NA-Leuko: All animal experiments were performed in accordance with the guidelines of the Animal Welfare Act and the Guide for the Care and Use of Laboratory Animals approved by The Houston Methodist Institutional Animal Care and Use Committee guidelines (Houston, TX, USA). 6–8 week-old Balb/c mice (Charles River Laboratories, Wilmington, MA, USA) were injected in the right ear with 10 μ L of LPS (5 mg mL⁻¹ solution, 50 μ g per ear). 100 μ L of rhodamine-labeled Leuko-NA was administered 30 min after LPS injection. Mouse ears (healthy and inflamed) were prepared for intravital microscopy (IVM) imaging at 1 and 24 h after injection to assess nanoparticles accumulation. Before IVM imaging, mice were injected with a 70 kDa FITC-dextran (50 μ L in PBS, Invitrogen) to identify the vasculature in the ear. IVM was performed with an upright Nikon A1R laser scanning confocal microscope equipped with a resonance scanner, motorized and heated stage, and Nikon long-working distance 4 \times and 20 \times dry Plan-Apochromat objectives and was housed within the Intravital Microscopy Core at Houston Methodist Research Institute.

Statistical Analysis: GraphPad statistical software (La Jolla, CA) was used to assess statistical significance between groups. Student's *t*-test and one-way ANOVA test were applied to compare differences between groups. A value of *p* = 0.05 was considered statistically significant. For inflamed ear targeting, unpaired two-tailed *t*-tests assuming both population have equal SD were used to compare means of fold change in accumulation at 1 and 24 h.

Supporting Information

Supporting Information is available from the Wiley Online Library or from the author.

Acknowledgements

M.E. and J.R.H. contributed equally to this work. The authors thank D. A. Engler, R. K. Matsunami, and the HMRI Proteomics Programmatic Core Laboratory for mass spectrometry analyses. The authors acknowledge

the Sealy Center for Structural Biology and Molecular Biophysics at the University of Texas Medical Branch at Galveston for providing research resources. This work was supported by grants RF-2010-2318372 and RF-2010-2305526 from the Italian Ministry of Health, William Randolph Hearst Foundation, The Regenerative Medicine Program Cullen Trust for Health Care (Project ID: 18130014), Brown Foundation (Project ID:18130011), the Hearst Foundation (Project ID: 18130017), the NIH/NCI and the Office of Research on Women's Health (Grant # 1R56CA213859), and Cancer Prevention and Research Institute of Texas (Project ID: RP170466) to E.T. The authors acknowledge the George J. and Angelina P. Kostas Charitable Foundation and CARIPARO Foundation Ricerca Pediatrica 2016–2018 Grant. HUVECs were purchased from ATCC (PCS-100-010). Human blood was obtained from the Houston Methodist Blood Bank (IRB ID: Pro00012800).

Conflict of Interest

The authors declare no conflict of interest.

Keywords

bioinspired approach, biomimicry, inflammation, membrane protein incorporation, microfluidics

Received: May 16, 2017
Revised: November 27, 2017
Published online:

- [1] I. C. Gebeshuber, B. Majlis, F. Aumayr, L. Neutsch, F. Gabor, presented at *Proc. of the Third Vienna International Conf. on Micro and Nanotechnology—Viennano09*, Vienna, Austria, March 2009.
- [2] a) R. A. Meyer, J. C. Sunshine, J. J. Green, *Trends Biotechnol.* **2015**, *33*, 514; b) E. Blanco, H. Shen, M. Ferrari, *Nat. Biotechnol.* **2015**, *33*, 941; c) A. Parodi, R. Molinaro, M. Sushnitha, M. Evangelopoulos, J. O. Martinez, N. Arrighetti, C. Corbo, E. Tasciotti, *Biomaterials* **2017**, *147*, 155; d) R. Molinaro, C. Corbo, M. Livingston, M. Evangelopoulos, A. Parodi, C. Boada, M. Agostini, E. Tasciotti, *Curr. Med. Chem.* **2017**, *24*, 1.
- [3] a) A. Parodi, N. Quattrocchi, A. L. Van De Ven, C. Chiappini, M. Evangelopoulos, J. O. Martinez, B. S. Brown, S. Z. Khaled, I. K. Yazdi, M. V. Enzo, *Nat. Nanotechnol.* **2013**, *8*, 61; b) R. Molinaro, C. Corbo, J. Martinez, F. Taraballi, M. Evangelopoulos, S. Minardi, I. Yazdi, P. Zhao, E. De Rosa, M. Sherman, A. De Vita, N. E. Toledano Furman, X. Wang, A. Parodi, E. Tasciotti, *Nat. Mater.* **2016**, *15*, 1037.
- [4] C.-M. J. Hu, L. Zhang, S. Aryal, C. Cheung, R. H. Fang, L. Zhang, *Proc. Natl. Acad. Sci. USA* **2011**, *108*, 10980.
- [5] C.-M. J. Hu, R. H. Fang, K.-C. Wang, B. T. Luk, S. Thamphiwatana, D. Dehaini, P. Nguyen, P. Angsantikul, C. H. Wen, A. V. Kroll, *Nature* **2015**, *526*, 118.
- [6] R. H. Fang, C.-M. J. Hu, B. T. Luk, W. Gao, J. A. Copp, Y. Tai, D. E. O'Connor, L. Zhang, *Nano Lett.* **2014**, *14*, 2181.
- [7] C.-M. J. Hu, R. H. Fang, J. Copp, B. T. Luk, L. Zhang, *Nat. Nanotechnol.* **2013**, *8*, 336.
- [8] a) C. Corbo, A. Parodi, M. Evangelopoulos, D. A. Engler, R. K. Matsunami, A. C. Engler, R. Molinaro, S. Scaria, F. Salvatore, E. Tasciotti, *Curr. Drug Targets* **2015**, *16*, 1540; b) M. Evangelopoulos, A. Parodi, J. O. Martinez, I. K. Yazdi, A. Cevenini, A. L. van de Ven, N. Quattrocchi, C. Boada, N. Taghipour, C. Corbo, B. S. Brown, S. Scaria, X. Liu, M. Ferrari, E. Tasciotti, *Biomaterials* **2016**, *82*, 168; c) R. Palomba, A. Parodi, M. Evangelopoulos, S. Acciardo, C. Corbo, E. de Rosa, I. K. Yazdi, S. Scaria, R. Molinaro, N. E. Furman, J. You, M. Ferrari, F. Salvatore, E. Tasciotti, *Sci. Rep.* **2016**, *6*, 34422;

- d) C. Corbo, W. E. Cromer, R. Molinaro, N. E. Toledano Furman, K. A. Hartman, E. De Rosa, C. Boada, X. Wang, D. C. Zawieja, M. Agostini, F. Salvatore, B. P. Abraham, E. Tasciotti, *Nanoscale* **2017**, 9, 14581.
- [9] a) C. Corbo, R. Molinaro, M. Tabatabaei, O. C. Farokhzad, M. Mahmoudi, *Biomater. Sci.* **2017**, 5, 378; b) C. Corbo, R. Molinaro, A. Parodi, N. E. T. Furman, F. Salvatore, E. Tasciotti, *Nanomedicine* **2016**, 11, 81; c) C. Corbo, R. Molinaro, F. Taraballi, N. E. T. Furman, M. B. Sherman, A. Parodi, F. Salvatore, E. Tasciotti, *Int. J. Nanomed.* **2016**, 11, 3049; d) M. P. Monopoli, C. Åberg, A. Salvati, K. A. Dawson, *Nat. Nanotechnol.* **2012**, 7, 779; e) A. Salvati, A. S. Pitek, M. P. Monopoli, K. Prapainop, F. B. Bombelli, D. R. Hristov, P. M. Kelly, C. Åberg, E. Mahon, K. A. Dawson, *Nat. Nanotechnol.* **2013**, 8, 137.
- [10] C. Corbo, R. Molinaro, F. Taraballi, N. E. Toledano Furman, K. A. Hartman, M. B. Sherman, E. De Rosa, D. K. Kirui, F. Salvatore, E. Tasciotti, *ACS Nano* **2017**, 11, 3262.
- [11] P. M. Valencia, O. C. Farokhzad, R. Karnik, R. Langer, *Nat. Nanotechnol.* **2012**, 7, 623.
- [12] L. Capretto, D. Carugo, S. Mazzitelli, C. Nastruzzi, X. Zhang, *Adv. Drug Delivery Rev.* **2013**, 65, 1496.
- [13] A. Jahn, W. N. Vreeland, M. Gaitan, L. E. Locascio, *J. Am. Chem. Soc.* **2004**, 126, 2674.
- [14] D. Liu, S. Cito, Y. Zhang, C. F. Wang, T. M. Sikanen, H. A. Santos, *Adv. Mater.* **2015**, 27, 2298.
- [15] A. Jahn, J. E. Reiner, W. N. Vreeland, D. L. DeVoe, L. E. Locascio, M. Gaitan, *J. Nanopart. Res.* **2008**, 10, 925.
- [16] a) E. Kastner, R. Kaur, D. Lowry, B. Moghaddam, A. Wilkinson, Y. Perrie, *Int. J. Pharm.* **2014**, 477, 361; b) E. Kastner, V. Verma, D. Lowry, Y. Perrie, *Int. J. Pharm.* **2015**, 485, 122; c) M. Guimarães Sá Correia, M. L. Briuglia, F. Niosi, D. A. Lamprou, *Int. J. Pharm.* **2016**, 516, 91.
- [17] S. Garg, G. Heuck, S. Ip, E. Ramsay, *J. Drug Target* **2016**, 24, 821.
- [18] A. D. Stroock, S. K. Dertinger, A. Ajdari, I. Mezic, H. A. Stone, G. M. Whitesides, *Science* **2002**, 295, 647.
- [19] a) B. S. Pattni, V. V. Chupin, V. P. Torchilin, *Chem. Rev.* **2015**, 115, 10938; b) Y. Perrie, E. Kastner, S. Khadke, C. B. Roces, P. Stone, in *Vaccine Adjuvants: Methods and Protocols* (Ed: C. B. Fox), Humana Press, New York, NY **2017**, p. 127; c) C. Walsh, K. Ou, N. M. Belliveau, T. J. Leaver, A. W. Wild, J. Huft, P. J. Lin, S. Chen, A. K. Leung, J. B. Lee, C. L. Hansen, R. J. Taylor, E. C. Ramsay, P. R. Cullis, *Methods Mol. Biol.* **2014**, 1141, 109.
- [20] D. Liu, S. Cito, Y. Zhang, C. F. Wang, T. M. Sikanen, H. A. Santos, *Adv. Mater.* **2015**, 27, 2298.
- [21] D. Cosco, D. Paolino, F. De Angelis, F. Cilurzo, C. Celia, L. Di Marzio, D. Russo, N. Tsapis, E. Fattal, M. Fresta, *Eur. J. Pharm. Biopharm.* **2015**, 89, 30.
- [22] C. Marianecci, F. Rinaldi, L. Di Marzio, M. Matriota, S. Pieretti, C. Celia, D. Paolino, M. Iannone, M. Fresta, M. Carafa, *Int. J. Nanomed.* **2014**, 9, 635.
- [23] a) C. Celia, F. Cilurzo, E. Trapasso, D. Cosco, M. Fresta, D. Paolino, *Biomed. Microdevices* **2012**, 14, 119; b) J. Liu, X.-f. Huang, L.-j. Lu, M.-x. Li, J.-c. Xu, H.-p. Deng, *J. Hazard. Mater.* **2011**, 190, 214; c) C. Marianecci, D. Paolino, C. Celia, M. Fresta, M. Carafa, F. Alhaique, *J. Controlled Release* **2010**, 147, 127.
- [24] B. T. Luk, L. Zhang, *J. Controlled Release* **2015**, 220, 600.
- [25] A. May, R. Pool, E. van Dijk, J. Bijlard, S. Abeln, J. Heringa, K. A. Feenstra, *Bioinformatics* **2014**, 30, 326.
- [26] M. Gagliardi, *Ther. Delivery* **2017**, 8, 289.
- [27] D. Dehaini, X. Wei, R. H. Fang, S. Masson, P. Angsantikul, B. T. Luk, Y. Zhang, M. Ying, Y. Jiang, A. V. Kroll, W. Gao, L. Zhang, *Adv. Mater.* **2017**, 29, 1606209.
- [28] S. Svenson, *Curr. Opin. Solid State Mater. Sci.* **2012**, 16, 287.
- [29] P. K. Dagur, J. P. McCoy, *Curr. Protoc. Cytom.* **2015**, 5.1, 1.